

# Racemic $\beta$ -Sheets as Templates for the Generation of Homochiral (Isotactic) Peptides from Aqueous Solutions of (*RS*)-Valine or -Leucine *N*-Carboxyanhydrides: Relevance to Biochirogenesis

Irina Rubinstein,<sup>[a]</sup> Gilles Clodic,<sup>[b]</sup> Gerard Bolbach,<sup>[b]</sup> Isabelle Weissbuch,<sup>[a]</sup> and Meir Lahav\*<sup>[a]</sup>

**Abstract:** As part of our program on biochirogenesis of homochiral peptides from racemic precursors, we report the feasibility of obtaining peptides with homochiral sequences composed of up to 25 residues of the same handedness in the polymerization of racemic valine or leucine *N*-carboxyanhydrides in aqueous solutions, as initiated by amines. The composition of the oligopeptides was determined by MALDI-TOF mass spectrometry, and the sequences of some of the heterochiral diastereoisomers were studied by MALDI-TOF MS/MS performed on samples in which the *S* enantiomers of

the monomer were tagged with deuterium atoms. The process comprises several steps: 1) a Markov mechanism of asymmetric induction in the early stages of the polymerization yields libraries of racemic oligopeptides enriched with isotactic diastereoisomers, together with oligopeptide sequences containing enantiomeric blocks of homochiral residues; 2) the short peptides self-assemble into racemic colloidal ar-

**Keywords:** chirality • oligopeptides • self-assembly • sheet structures • template synthesis

chitectures that serve as regio-enantioselective templates in the ensuing process of chain elongation; 3) homochiral residues of the amino acids located at the periphery of these colloidal aggregates exert efficient enantioselection, which results in the formation of long isotactic oligopeptides. The final diastereoisomeric distribution of the peptides depends upon the composition of the templates, which is determined by the concentration of the initiator. The racemic mixtures of isotactic peptides can be desymmetrized by using enantiopure methyl esters of  $\alpha$ -amino acids as initiators.

## Introduction

One of the open questions about the origin of life deals with the timing and possible scenarios that might have been responsible for the emergence of homochiral biopolymers in the achiral prebiotic environment. Two central surmises have been proposed: one suggests that homochirality emerged after the development of the primeval biological system,<sup>[1]</sup> whereas the second maintains that enantiomeri-

cally pure compounds are a prerequisite for the evolution of living species and that “mirror-symmetry breaking” must have taken place before the emergence of life.<sup>[2–6]</sup> In the absence of reliable fossils, it is difficult to track down this historical event; however, by performing laboratory experiments, one may cast light on possible reaction pathways that demonstrate the feasibility of converting racemic activated monomers of amino and nucleic acids into homochiral biopolymers. Such a scenario involves two central problems: first, the production of long polymeric chains composed from residues of the same handedness (isotactic chains) by starting from racemic reagents and overriding the difficulties of binomial kinetics in the polymerization of multicomponent monomers in an isotropic medium; second, the achievement of mirror-symmetry breaking in the racemic mixtures of isotactic peptides.

Previously, a number of models have been proposed to highlight the problem of biochirogenesis of peptides on Earth, including those by Bonner and co-workers,<sup>[7]</sup> by Brack,<sup>[8]</sup> and by Luisi and co-workers.<sup>[9,10]</sup>

[a] Dr. I. Rubinstein, Dr. I. Weissbuch, Prof. Dr. M. Lahav  
Department of Materials and Interfaces  
The Weizmann Institute of Science  
76100 Rehovot (Israel)  
Fax: (+972)8934-4138  
E-mail: meir.lahav@weizmann.ac.il

[b] G. Clodic, Dr. G. Bolbach  
Plate-Forme Spectrométrie de Masse et Protéomique  
Université Pierre et Marie Curie  
75252 Paris Cedex 05 (France)

In our approach, we have followed a working hypothesis that comprises several steps: the formation of libraries of short oligomers composed from blocks of homochiral sequence, followed by the self-assembly of the oligomers through hydrogen bonding into aggregates that operate as regio-enantiospecific templates and control the ensuing process of chain elongation.<sup>[11–15]</sup> Such a scenario has common features with the process of crystallization, which comprises the steps of crystal nucleation and stereospecific growth.

Herein, we report a regio-enantioselective process in the polymerization of *N*-carboxyanhydrides of racemic leucine (Leu-NCA) or valine (Val-NCA) in aqueous solution to yield isotactic oligopeptides.

## Results

Polymerization of racemic Val-NCA or Leu-NCA, enantioselectively tagged with 8 and 10 deuterium atoms, respectively, was performed in aqueous solution by dissolving the monomer in water and, after 5 min for the first system and 1 min for the second, adding 5, 10, or 25% (mol/mol) of initiator, namely *n*-butylamine or enantiopure methyl ester of Val (Val-OMe), Leu (Leu-OMe), or phenylalanine (Phe-OMe), under a continuous vortex. The reaction started at room temperature as a clear solution; however, foam appeared after 30 s to a few minutes, due to CO<sub>2</sub> evolution, and the solution became turbid as a result of the formation of colloidal peptide aggregates. The X-ray diffraction patterns of these colloids were measured, either in situ with the aqueous solution in a capillary, as shown for racemic Val-NCA initiated by *n*-butylamine in Figure 1a, or at the end of the reaction after centrifugation, water decantation, and drying (Figure 1b, c). These patterns are very similar, are independent of the concentration of the initiator, and display Bragg peaks at *d* spacings of 4.7 Å for both the Val and Leu oligopeptides, indicative of interchain hydrogen bonding between the peptide bonds, and of 9.7 and 12 Å for oligo-Val and oligo-Leu, respectively, indicative of the peptide interlayer spacing. The dry oligopeptides also displayed a *d* spacing of 6.9 Å, which corresponds to an extended peptide backbone.

The FTIR spectra of both systems showed the C=O amide I stretching-vibration band at  $\tilde{\nu}=1633\text{ cm}^{-1}$  and the N–H amide II band at  $\tilde{\nu}=1540\text{ cm}^{-1}$ . The XRD and FTIR measurements are in keeping with the formation of  $\beta$ -sheet-like structures that are stacked in architectures through the hydrophobic side groups. Additional evidence is provided by AFM images (for example, Figure 2) of the colloidal aggregates formed after  $\approx 10$  min of polymerization and deposited on a mica support. The morphology appears filament-like, of 40–60 nm in width, and with thicknesses in the range of 1.0–2.8 nm.

The MALDI-TOF mass spectra of the oligopeptides obtained from the polymerization of racemic Val-NCA with 25, 10, and 5% (mol/mol) of *n*-butylamine initiator are shown in Figure 3a–c. In the spectra, the isotactic oligopepti-

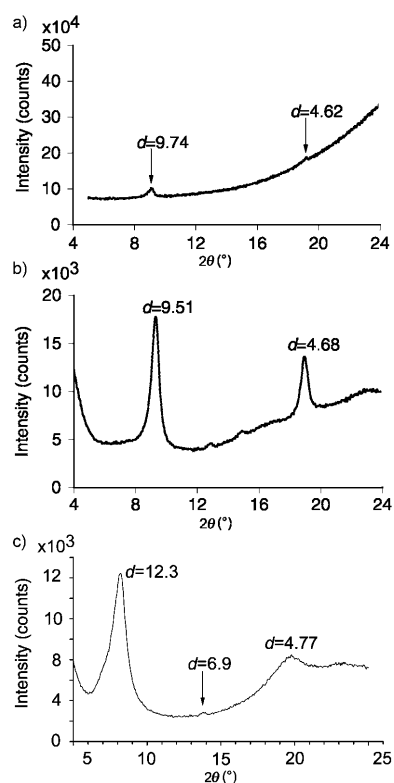


Figure 1. X-ray powder diffraction patterns measured from a) a heterogeneous reaction mixture of (*RS*)-Val-NCA initiated with 25% (mol/mol) *n*-butylamine inserted in a capillary; b and c) the water-insoluble oligopeptides obtained in the polymerization of (*RS*)-Val-NCA and (*RS*)-Leu-NCA, respectively, with 25% (mol/mol) *n*-butylamine.

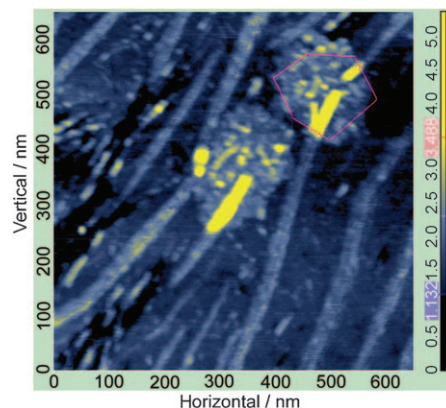


Figure 2. AFM image of the colloidal architectures formed after 10 min of polymerization of (*RS*)-Val-NCA in an aqueous solution in the presence of *n*-butylamine and subsequent transfer to a mica support.

des, (of homochiral sequence), labeled  $R_n$  and  $S_n$ , are located at the wings of each group of signals originating from various diastereoisomers of a given length  $n$ , whereas those peptides containing heterochiral residues, labeled  $R_nS_d$  in which  $h+d=n$ , are located between them. In our previous studies, we have demonstrated that the molar fractions of the diastereoisomeric oligopeptides of a given length are

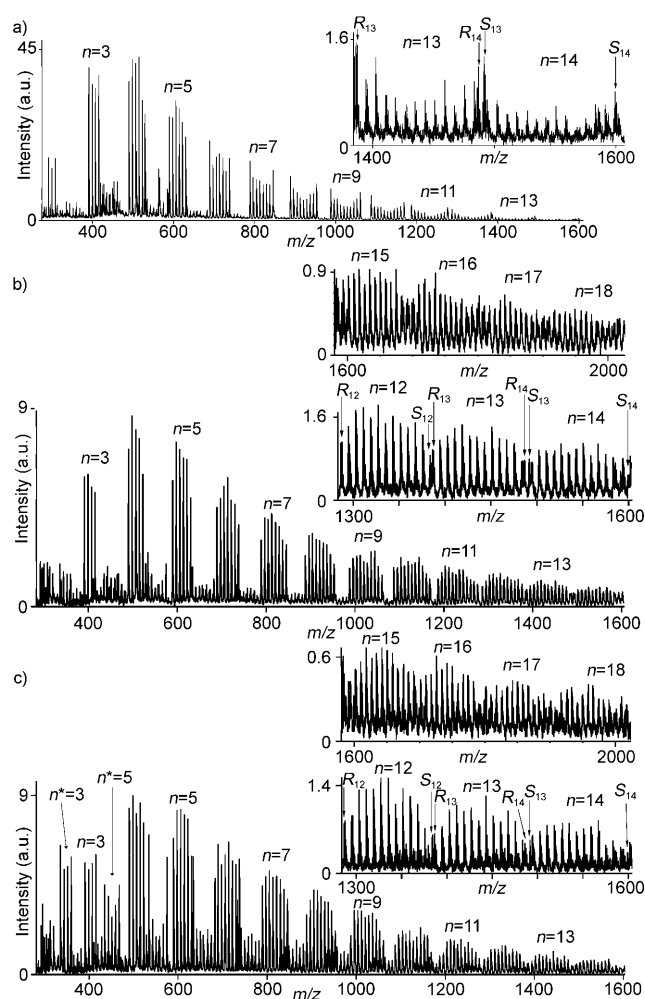


Figure 3. MALDI-TOF MS analysis of the  $\text{Na}^+$ -cationized oligopeptides obtained from the polymerization of racemic Val-NCA initiated with *n*-butylamine at a) 25, b) 10, and c) 5% (mol/mol). Oligopeptides initiated by traces of water are labeled with \*.

proportional to the relative intensities of their signals. Therefore, one can clearly deduce from the spectra in Figure 3 that the diastereoisomeric distribution of the oligopeptides strongly depends on the concentration of initiator used in the reaction. The signal intensities corresponding to the isotactic oligopeptides increase significantly, in comparison with those of their heterochiral counterparts, with an increase in the amount of initiator. The common feature of these spectra is that the short peptides comprise all possible diastereoisomers in similar molar fractions, independent of the concentration of initiator. On the other hand, the molar fractions of the isotactic diastereoisomers beyond the heptamers (7–14-mers) and of those containing one heterochiral residue, labeled ( $n-1$ ) and ( $1-n$ ), increase with length. This result significantly departs from the binomial distribution for either the Val or Leu reaction systems.

Histograms of the molar fractions (Figure 4), calculated from the signal intensities in the mass spectra, show the distribution of the diastereoisomers of each length  $n$  obtained in the polymerization of racemic Val-NCA in water with 25

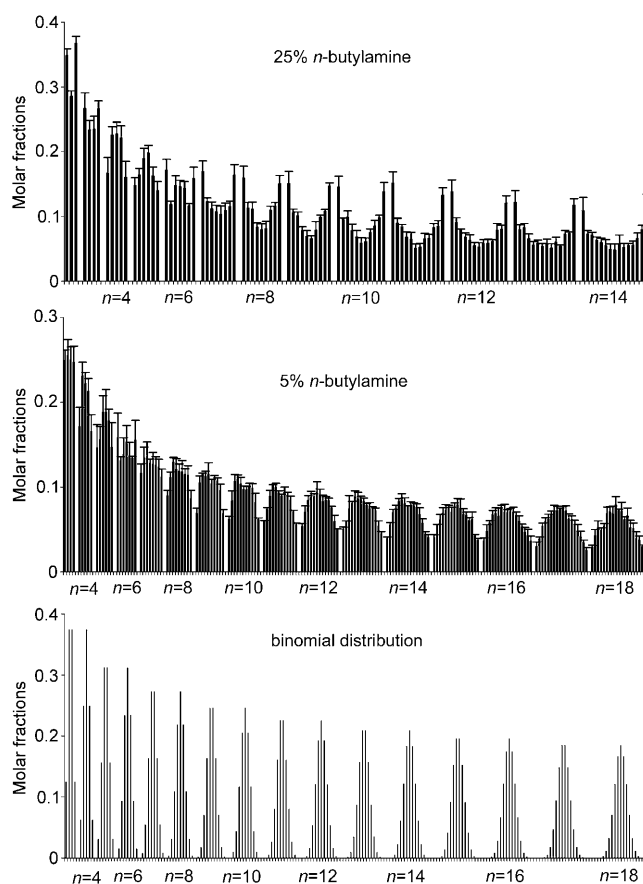


Figure 4. Histograms showing the distribution of the diastereoisomers of each length  $n$  obtained in the polymerization of racemic Val-NCA in water as initiated by *n*-butylamine at a) 25 and b) 5% (mol/mol). c) Histogram showing the calculated values with assumption of a binomial distribution of the diastereoisomers.

and 5% (mol/mol) of *n*-butylamine initiator, along with the corresponding values calculated for a theoretical binomial distribution. At 25% initiator, the isotactic peptides are the most dominant diastereoisomers for longer oligopeptides comprising 7–14 residues (Figure 4a). At 5% initiator, the mole fractions of the isotactic peptides appear to be somewhat smaller than those of the corresponding heterochiral ones, (Figure 4b); however, they are significantly higher than those calculated by assuming a theoretical binomial distribution (Figure 4c). The observed peptide distribution implies the operation of enantioselection in the chain-elongation process.

The MALDI-TOF mass spectra of oligopeptides obtained in the polymerization of racemic Leu-NCA in THF and water with *n*-butylamine initiator are shown in Figure 5. In the organic solvent, the reaction takes place under homogeneous conditions.<sup>[16]</sup> The isotactic di- and tripeptides are formed more commonly than in a random process (Figure 5a) as a result of the operation of a Markov mechanism, by which a homochiral residue at the N terminus of the peptide chain adds preferentially, upon reaction, another amino acid residue of the same handedness.<sup>[9,10]</sup> Such partial asym-

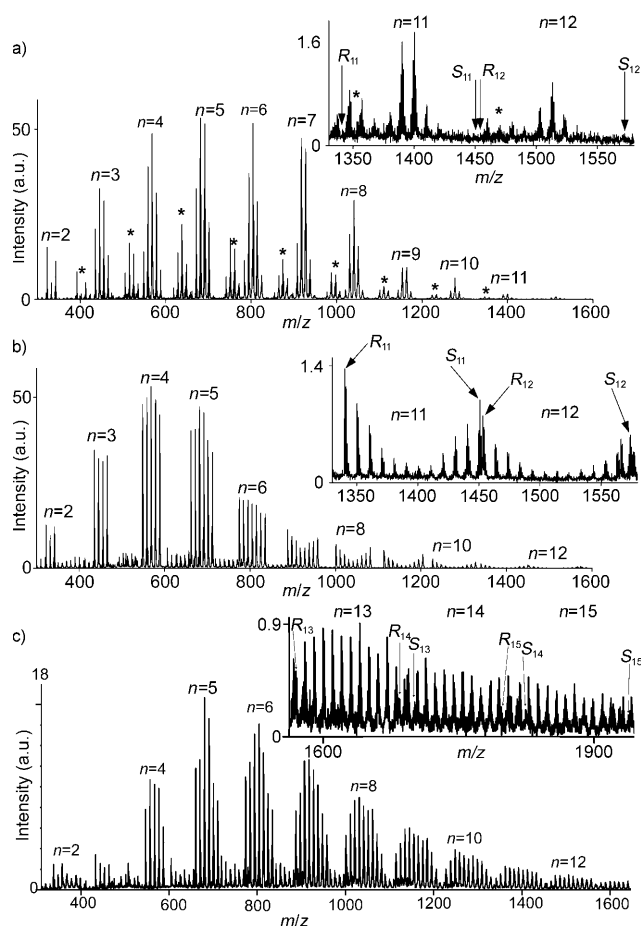


Figure 5. MALDI-TOF MS analysis of the oligopeptides obtained from polymerization of racemic Leu-NCA a) in THF with 25% (mol/mol) of *n*-butylamine; b and c) in water with 25 and 10% (mol/mol) of *n*-butylamine, respectively. Oligopeptides initiated by traces of water are labeled with \*.

metric induction introduced by isolated chains should drive the reaction towards random diastereoisomeric distribution of the long oligopeptide chains. By contrast, the distribution of the longer oligopeptides obtained by polymerization in water (Figure 5b and c) shows a significant departure from the random distribution. This difference in the diastereoisomeric distribution of the oligopeptides in the two solvents suggests the occurrence of self-assembly of the short hydrophobic isotactic and atactic oligopeptides into clusters in water, but not in the organic solvent; these clusters then operate as templates and induce regio-enantioselection in the later stages of the reaction.

The homochiral enhancement obtained in the polymerization of racemic Val-NCA initiated with 25 and 5% (mol/mol) of *n*-butylamine was evaluated by dividing the experimental molar fractions of isotactic oligopeptides of each length with those calculated for a theoretical binomial distribution (Figure 6). Thus, the homochiral enhancement for dodecapeptides has a value of 550 at 25% initiator and only 200 at 5% initiator, but it increases to  $\approx 7000$  for the 18-mer peptides.

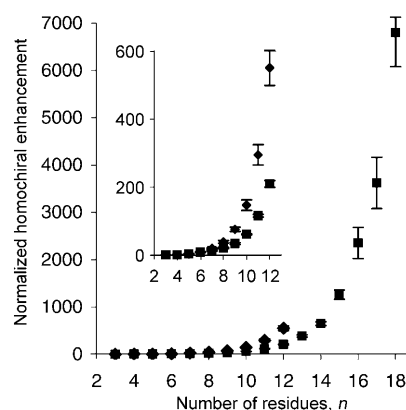


Figure 6. Plot of the normalized homochiral enhancement of the isotactic oligo-Val chains of various lengths *n* obtained with 25 (♦) and 5% (mol/mol) (■) of *n*-butylamine. The insert shows a magnified plot for *n*=2–7.

Some of the short peptides are water-soluble, as shown by the MALDI-TOF MS of the supernatant solution after removal of the water-insoluble fraction (Figure 7a–c). The water-soluble fraction contains primarily the di- and tripeptide diastereoisomers and only heterochiral tetra- to hexapeptides, whereas the isotactic penta- and hexapeptides are water insoluble. The importance of this result is considered in the discussion of the mechanism of the reaction (see below).

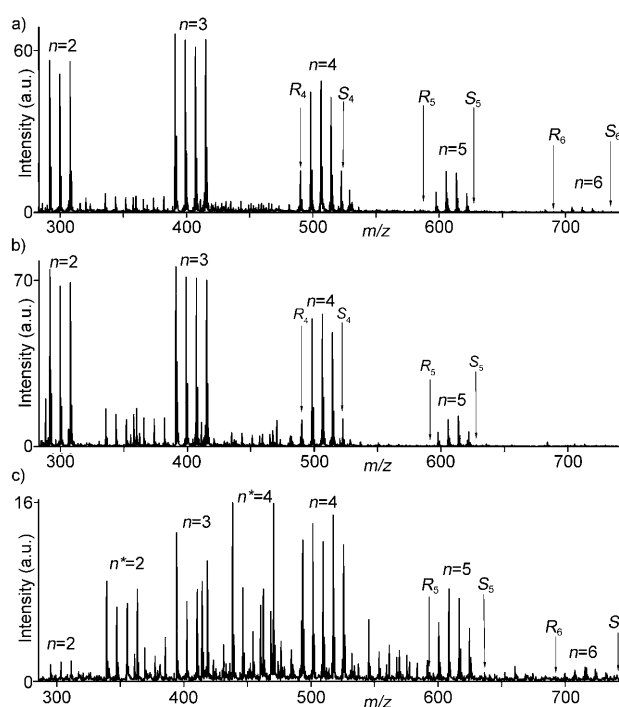


Figure 7. MALDI-TOF spectra of the water-soluble oligopeptides obtained from the polymerization of racemic Val-NCA in water with a) 25, b) 10, and c) 5% (mol/mol) *n*-butylamine initiator. Isotactic oligopeptides are marked arrows and labeled  $R_n$  or  $S_n$ . Oligopeptides initiated by traces of water are labeled with \*.

To obtain additional insight into the sequences of the heterochiral peptides, they were analyzed by MALDI-TOF-TOF MS. In this analysis, fragmentation of the ions by a metastable decomposition and/or collision-induced dissociation showed two main fragmentation series (see the Experimental Section). Data analysis shows that the  $n$ -butylamine initiator (I), located at the C terminus, is linked to  $R$  or  $S$  residues. For the heterochiral oligopeptides, at 25% initiator, the fragmentation studies clearly highlight the presence of a block sequence. Typically, for  $n=6$ , the overexpressed sequences (N to C terminus) were  $SRRRRR-I$  and  $RRRRRS-I$  for (5,1),  $SSRRRR-I$  and  $RRRRSS-I$  for (4,2),  $RRSSSS-I$  and  $SSSSRR-I$  for (3,3),  $RRSSSS-I$  and  $SSSSRR-I$  for (2,4), and  $RSSSSS-I$  and  $SSSSSR-I$  for (1,5). The single residue of opposite handedness for the oligopeptides labeled  $(n-1,1)$  and  $(1,n-1)$ , in which  $n=4-9$ , is located at either the N or the C terminus of the chains. Similarly, for the oligopeptides comprising two residues of opposite handedness, labeled  $(n-2,2)$  and  $(2,n-2)$ , the sequence has two blocks grouping residues of same handedness. For longer oligopeptides,  $n > 7$ , with a similar number of  $R$  and  $S$  residues, blocks of 2-4 residues of the same handedness were observed.

A more complex picture was observed for MALDI-TOF-TOF analysis of heterochiral peptides obtained in the polymerization of  $(RS)$ -Val-NCA with 10 or 5%  $n$ -butylamine. The oligopeptides bearing one heterochiral residue,  $(n-1,1)$  and  $(1,n-1)$  in which  $n=5-9$ , showed this residue in a rather random location. For the diastereoisomers that contain more than one residue of opposite handedness, smaller blocks of 2 or 3 residues of the same handedness were found, in contrast to the results obtained with 25% initiator.

**Desymmetrization of the racemic mixtures:** In our attempts to desymmetrize the racemic mixtures of the isotactic peptides, we performed the polymerization reactions with the methyl esters of Val, Leu, or Phe of either absolute configuration. The distributions of the diastereoisomeric oligopeptides obtained in the polymerization of racemic Val-NCA with 25, 10, and 5%  $S$ -Val-OMe are shown in Figure 8 and the corresponding results for racemic Leu-NCA with 25, 10, and 5%  $S$ -Leu-OMe are in Figure 9. The enantiomeric excess ( $ee$ ) values of the isotactic peptides as a function of length for the Val and Leu systems with 25% initiator are shown in Figure 10 (left). From these plots, we notice that the enantiopure initiator engenders asymmetric induction in the initiation of the polymerization and the  $ee$  value decreases around the tetramer-hexamer region. Beyond this length, a reversal in the  $ee$  value occurs, such that the oligopeptide chains composed from residues of the opposite handedness to that of the initiator are formed in excess. Note that, by symmetry,  $S$ - and  $R$ -Val-OMe yielded mirror-symmetry-related results.

When the polymerization of either racemic Leu-NCA or racemic Val-NCA was initiated with 10 or 5% methyl ester, the di- to hexapeptides were formed with an excess of chains composed from residues with the same absolute con-

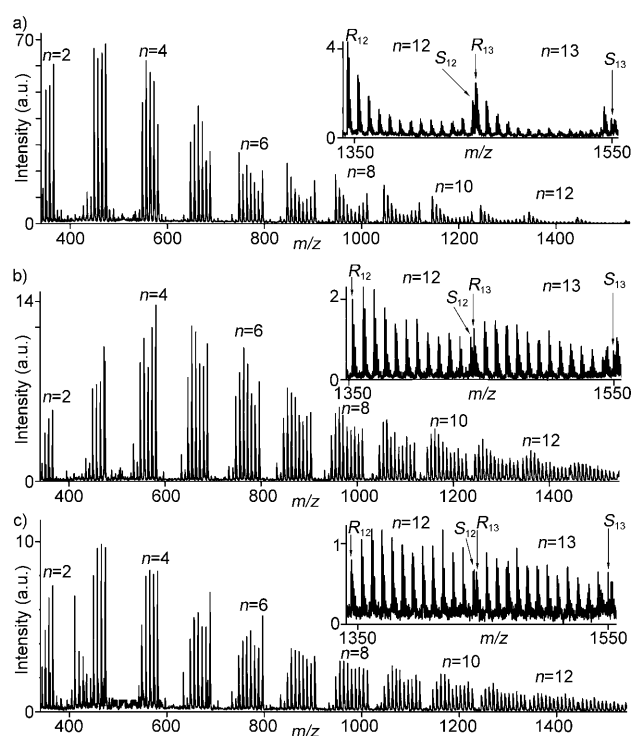


Figure 8. MALDI-TOF MS analysis of the  $Na^+$ -cationized oligopeptides obtained from the polymerization of racemic Val-NCA initiated with  $S$ -Val-OMe at a) 25, b) 10, and c) 5% (mol/mol).

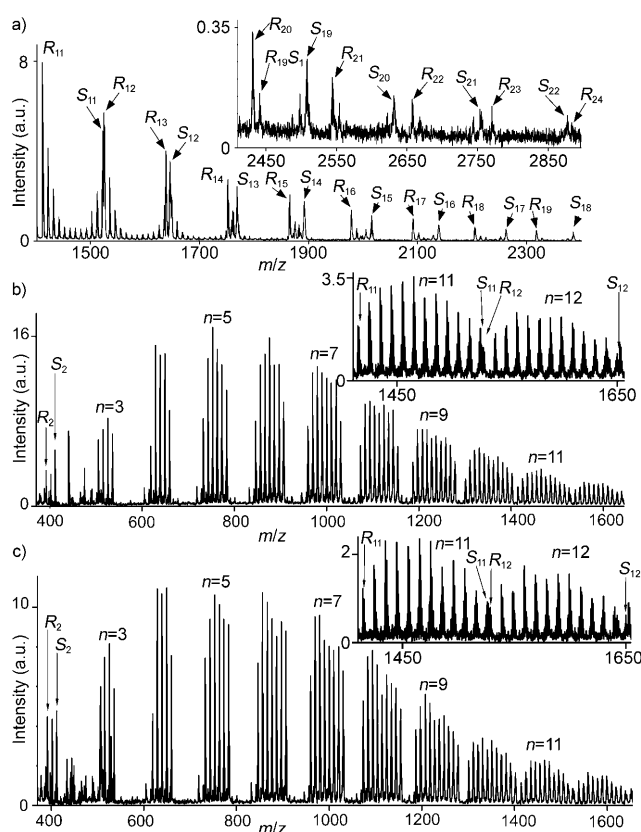


Figure 9. MALDI-TOF MS analysis of the  $Na^+$ -cationized oligopeptides obtained from the polymerization of racemic Leu-NCA initiated with  $S$ -Leu-OMe at a) 25, b) 10, and c) 5% (mol/mol).

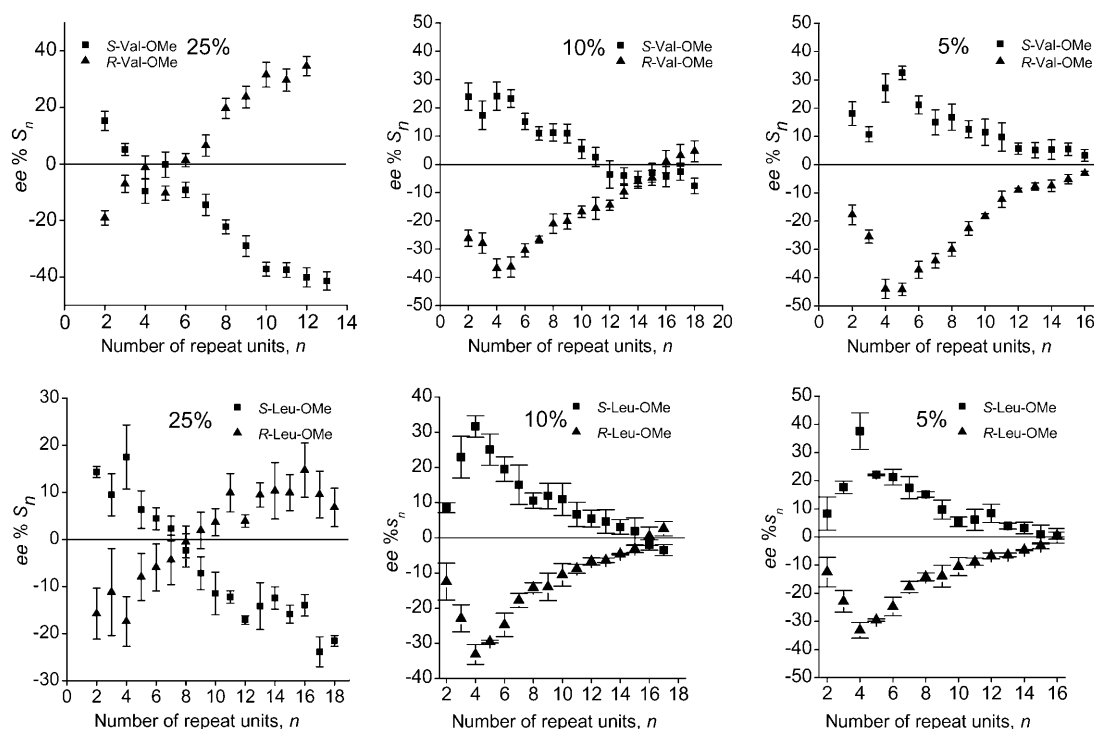


Figure 10. Plots of  $ee\% S_n = 100([S_n] - [R_n]) / ([S_n] + [R_n])$  of the isotactic oligopeptides for each length  $n$  obtained from the polymerization of racemic Val-NCA (top) and racemic Leu-NCA (bottom) in water with 25, 10, or 5% (mol/mol) of *R* initiator ( $\blacktriangle$ ) or *S* initiator ( $\blacksquare$ ). Error bars are the average of five samples.

figuration as the initiator. The *ee* value increases for the tetra- to hexapeptides and then it decreases slowly to almost racemic composition (Figure 10, middle and right).

The polymerization of racemic Leu-NCA with 25% *R*- or *S*-Leu-OMe initiator (Figure 9a) demonstrates the formation of detectable isotactic peptides of 25 residues in length. The distribution of the short peptides is comparable to that obtained from racemic Val-NCA; however, the peptides formed beyond the hexa- and heptamers are primarily isotactic oligopeptides or those containing one residue of opposite handedness (Figure 9a), which, according to the MALDI-TOF MS/MS analysis, is located either at the N terminus or adjacent to the initiator at the C terminus of the peptide chains.

## Discussion

The feasibility of forming racemic mixtures of oligopeptides of homochiral sequence, of up to 25 residues, during polymerization in aqueous solutions of racemic Leu-NCA and Val-NCA has been demonstrated. These isotactic peptides are formed in concentration orders of magnitudes higher than those anticipated from a random polymerization reaction. Moreover, the racemic mixtures of isotactic peptides could be desymmetrized if the polymerization was initiated by enantiopure methyl esters of  $\alpha$ -amino acids.

The mechanism of this reaction is very complex because it starts and proceeds in its early stages under homogeneous

conditions. Once the tetra-, penta-, and hexapeptides have been formed, they self-assemble into water-insoluble colloidal aggregates, such that the ensuing process of chain elongation continues heterogeneously at the colloidal-particle/solution interface. Nevertheless, in spite of this complication, one may outline some of the mechanistic details of the reaction by analyzing, by mass spectrometry, the final composition of the diastereoisomeric oligopeptides and the sequences of some of the chains containing heterochiral residues.

**Stereospecific templates from oligopeptides comprising enantiomeric blocks:** The MALDI-TOF MS analysis of whole reaction mixtures shows that the di-, tri-, and tetramers are enriched with isotactic diastereoisomers composed of residues of the same handedness (Figure 4), in comparison with a random distribution. This result implies that the  $\text{NH}_2$  end group of the ultimate homochiral amino acid exerts asymmetric induction in the early stages of the chain-propagation process, which occurs in the isotropic solution, by preferentially selecting residues of the same handedness. The short peptides are water soluble, as indicated by the MALDI-TOF MS analysis of the aqueous solution after removal of the precipitate (Figure 7).

The relative composition of the short peptides and their solubility in water determines the structure and chemical properties of the colloidal self-aggregates that operate as templates in the formation of the longer peptides. By changing the concentration of the initiator, one varies the diaste-

reoisomeric composition of the short peptides, and consequently, the composition and chemical properties of the colloidal aggregates. When 5 or 10% initiator is used, peptides longer than 25 residues were observed. The diastereoisomeric libraries are composed from complex mixtures of isotactic and atactic peptides. Nevertheless, the relative composition of the longer peptides as a function of length indicates that they depart significantly from a theoretical random distribution (Figure 4b and c). Thus, with 5% initiator, the normalized homochiral enhancement, defined as the molar fraction of isotactic peptides normalized to those for random polymerization (Figure 6) increases with chain length and reaches a value of  $\approx 7000$  for the 18-mer isotactic peptides. In addition, the relative composition of the isotactic versus heterochiral diastereoisomeric peptides decreases only slightly as a function of chain length. The histograms of

the diastereomeric distribution of the polymerization products of racemic Val-NCA in water initiated by 5% *n*-butylamine (Figure 4b) suggest that the reaction assumes a regio-antioselective pathway beyond a certain length and that most of the heterochiral residues are inserted in the chains in the early stages of the polymerization and are thus primarily located close to the C terminus of the peptide chains. Further support for this model is obtained from the MALDI-TOF-TOF MS/MS results for the oligopeptides obtained in the polymerization of racemic Val-NCA initiated by 10% *S*-Val-OMe, as represented by an evolving tree of penta- to undecapeptides (amenable to the analysis) in Figure 11. The oligopeptides composed from homochiral residues,  $S_5-I_S$  and  $R_5-I_S$ , evolved into longer isotactic ones,  $S_{11}-I_S$  and  $R_{11}-I_S$ , but also into oligopeptides composed mainly from two blocks of homochiral sequences. All of the shortest heterochiral sequences present in the insoluble fraction have the two-block sequence with *S* residues linked to  $I_S$  ( $R-SSSS-I_S$ ,  $RR-SSS-I_S$ ,  $RRR-SS-I_S$ , and  $RRRR-S-I_S$ ) and they evolved into heterochiral sequences containing two blocks of opposite handedness, such as  $RRRRRR-SSSS-I_S$ ,  $RRRRRRRR-SSS-I_S$ ,  $RRRRRRRR-SS-I_S$ , and  $RRRRRRRRRR-S-I_S$ . One notices that, as a result of the asymmetric induction of the *S* initiator, the formation of short chains containing an excess of *S* residues close to the initiator is favored. When these long blocks react with an

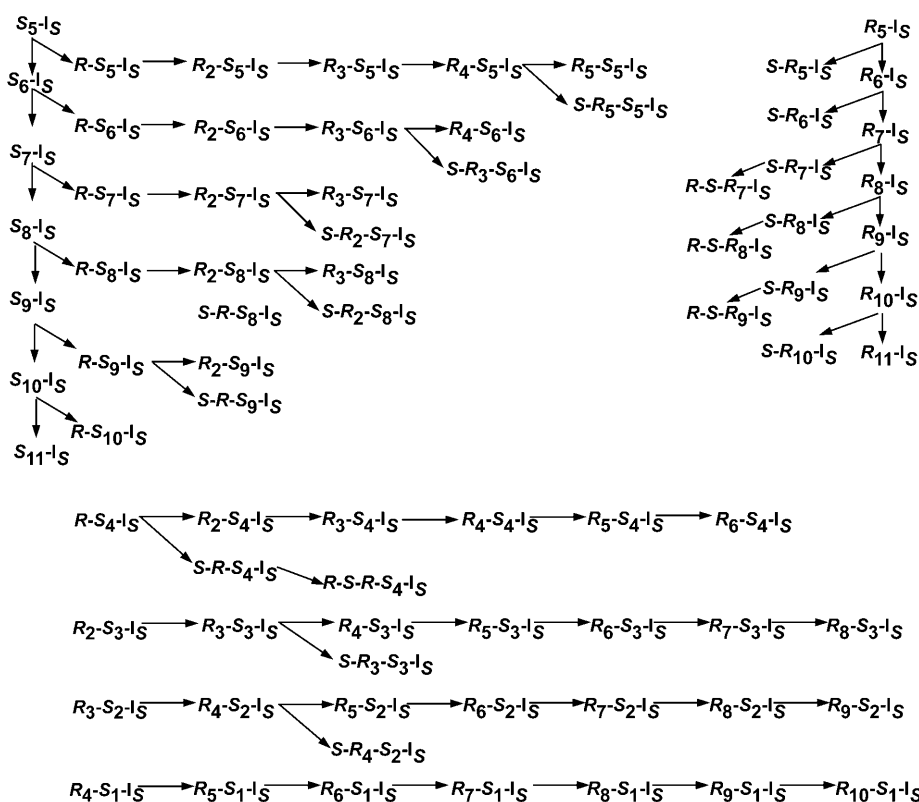


Figure 11. Schematic representation of the evolution of the most representative sequences of pentapeptide diastereoisomers as suggested by MALDI-TOF-TOF MS data analysis of the products obtained from the polymerization of racemic Val-NCA initiated with 10% (mol/mol) *S*-Val-OMe.

amino acid of opposite handedness, they either undergo chain termination or, presumably, form an additional block.

On the basis of these results, we propose that, once a library of short racemic oligopeptides composed of short blocks of enantiomeric residues is formed, the oligopeptides self-assemble into colloidal templates. The FTIR spectra and X-ray diffraction patterns measured from these templates suggest the formation of  $\beta$ -sheet-like architectures, due to hydrogen-bond formation between chains composed of short homochiral blocks of opposite handedness and sheet stacking through hydrophobic contacts. Although the composition of these colloidal particles is racemic, all of the chains expose  $NH_2$  end groups of homochiral amino acid residues of either handedness to the periphery. As a result of the asymmetric induction exerted by these groups, the process of chain elongation continues to be regio-antioselective. The newly formed isotactic blocks on the surfaces of the colloidal templates can continue to self-assemble between themselves or with short peptides from the solution to yield more robust sheets.

**Rippled  $\beta$ -sheets as templates for the formation of isotactic peptides:** To increase the concentration of longer isotactic oligopeptides, it was imperative to find conditions under which one may generate, at an early stage of the reaction, colloidal templates that are composed primarily from short



isotactic oligopeptides. The analysis of the water-soluble fractions of the polymerization of racemic Leu-NCA and racemic Val-NCA demonstrates that the isotactic tetra- to hexapeptides (Figure 7) were less soluble than the heterochiral oligopeptides. Consequently, if enhanced concentrations of these isotactic peptides are obtained during the early stages of polymerization, one can design polymerization conditions whereby these peptides can separate from the others as ordered  $\beta$ -sheet templates that can promote the formation of long isotactic peptides. Indeed, when the reaction was performed with 25% enantiopure Val-OMe or Leu-OMe, we obtained isotactic peptides and those that contained one residue of opposite handedness attached to the initiator as the dominant diastereoisomers.

The powder X-ray diffraction, AFM, and FTIR measurements cannot differentiate, within these colloidal particles, between parallel (*p*) and antiparallel (*ap*)  $\beta$ -sheets or between racemic and pleated sheets. The racemic (rippled)  $\beta$ -sheets might be more favored for kinetic and thermodynamic reasons. In kinetic terms, provided that the rippled and pleated sheets are of the same stability, the rate of self-assembly of racemic  $\beta$ -sheet aggregates should depend upon the concentrations of the *S* and *R* chains, whereas the formation of the enantiomorphous pleated sheets, because they are thermodynamically separated phases, should depend upon the concentration of only one of the enantiomers (Figure 12).

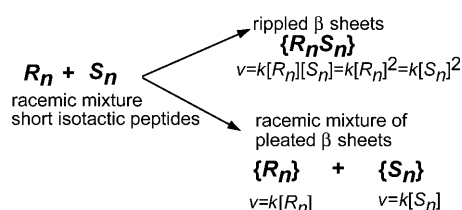
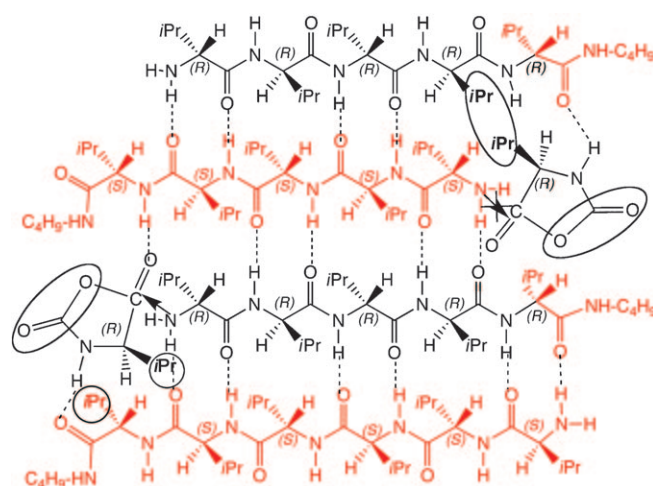


Figure 12. Schematic representation of the self-assembly of a racemic mixture of short isotactic peptides into either rippled  $\beta$ -sheets or racemic mixtures of enantiomorphous pleated  $\beta$ -sheets.

The rippled  $\beta$ -sheets are composed of alternating isotactic peptide chains of opposite handedness. Indeed, Pauling and Corey demonstrated the possibility of the formation of such  $\beta$ -sheets.<sup>[17]</sup> Support for the proposed structures of our templates is also provided by the racemic rippled *ap*  $\beta$ -sheets observed in the crystal structures of the glycine tripeptide<sup>[18]</sup> and the high-molecular-weight polyglycine I polymorph.<sup>[19–21]</sup> These achiral peptides of glycine have the option of crystallizing in the form of either pleated or racemic  $\beta$ -sheets and they prefer to form the racemic rippled *ap*  $\beta$ -sheet motif. Another reported example is a solubility study showing that the mixing of equal amounts of water-soluble polylysine of opposite handedness results in the precipitation of the racemate.<sup>[22,23]</sup>

The formation of rippled *ap*  $\beta$ -sheets and rippled *p*  $\beta$ -sheets has been reported in the polymerization of racemic crystals of (*RS*)-Phe-NCA<sup>[11,12,24]</sup> and (*RS*)-Val-NCA,<sup>[13]</sup> re-

spectively, suspended in an organic solvent or water containing the initiator. On the other hand, NMR spectroscopy studies of short racemic oligopeptides forming  $\beta$ -sheet-like architectures in chloroform have shown that the interactions between residues residing in neighboring chains of the same handedness are more stable than those of opposite handedness by 0.6–0.8 kcal per residue.<sup>[25]</sup> Consequently, it is of interest to prove experimentally the structure of the  $\beta$ -sheet templates under the present reaction conditions. For this purpose, we took advantage of the structural differences between the various motifs. Homochiral rims delineate the rippled  $\beta$ -sheet templates and, therefore, they can induce regio-enantioselection in the formation of the longer peptides. Such enantioselection can be shown schematically for the arrangement of the NCA monomer molecules at the growing enantiomeric sites of the template. An NCA molecule of *R* configuration can react enantioselectively with the  $\text{NH}_2$  group of an *R* chain, with assistance in the transition state from two hydrogen bonds, one between the to-be-reacted C=O carbonyl group and an N–H group of a neighboring *S* chain and the second between the N–H group of the NCA molecule and the C=O bond of the amide C-terminal end group of a different neighboring *S* chain (Scheme 1). Such interactions will organize the NCA monomer molecule with the alkyl group away from the surface of the template and will bring the to-be-reacted C=O group into a proper orientation to form a new residue of the same absolute configuration as that of the growing peptide chain. Such a transition state should reduce the energy of activation in comparison with that of the reaction of an NCA monomer molecule with an isolated peptide chain. At the same time, if an *R*-NCA molecule approaches the  $\text{NH}_2$  reactive group of an *S* chain, as required for chain elongation, it will sense steric hindrance between its *i*Pr group and the *i*Pr group of an adjacent *R* chain (Scheme 1).



Scheme 1. Schematic representation of an *R*-Val-NCA molecule interacting with the  $\text{NH}_2$  end group of an *R* chain (in black) and an *S* chain (in red) confined in a rippled *ap*  $\beta$ -sheet template. These interactions account for the enantioselectivity of the chain-elongation process.



Experimental support for the preferred formation of rippled *ap*  $\beta$ -sheets, rather than a racemic mixture of pleated sheets, could be obtained from the reversal in the *ee* value of the oligopeptide chains as a function of length when enantiopure initiators are used. Such polymerization initiators should yield different diastereoisomeric oligopeptides according to different possible motifs, as illustrated schematically in Figure 13.

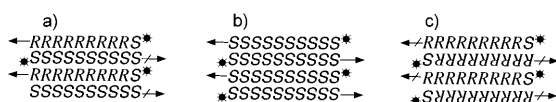


Figure 13. Different types of *ap*  $\beta$ -sheets comprising four strands of homochiral sequences with an  $S^*$  residue of the initiator attached at the C terminus. a) Racemic  $\beta$ -sheet of alternating oligo-*R* and oligo-*S* strands, in which the  $S^*$  residue of the initiator is attached to the oligo-*R* chains and impedes the growth of adjacent *S* chains. b and c) Enantiomorphous pleated  $\beta$ -sheets of either oligo-*S* or oligo-*R* strands: b) The  $S^*$  initiator attached to the oligo-*S* chains in a pleated motif will not hinder the growth of chains of the same absolute configuration as that of the initiator; c) the  $S^*$  residue is attached to the C terminus of the oligo-*R* chains and should hinder the growth of these chains. The horizontal arrows represent the direction of chain elongation and the inclined lines represent sites where the  $S^*$  initiator residue impedes the growth of adjacent strands

The analysis of the architectures in Figure 13 suggests that, if the reaction is initiated by an enantiopure methyl ester of, say, *S* absolute configuration, this residue will reside at the C terminus of isotactic peptide chains composed from repeat homochiral residues of either handedness. Such a residue will be integrated coherently within the chains composed of *S* residues and will not interfere with the growth of the nearer peptide chains comprising *R* residues (Figure 13a). On the other hand, the presence of the same initiator at the C terminus of an *R* chain creates a defect at the rim of the growing template. In the case of a racemic *ap*  $\beta$ -sheet (Figure 13a), such an initiator residue will introduce steric hindrance to the growing  $\text{NH}_2$  group of the neighboring peptide chains composed from *S* residues, which will result in an excess of the isotactic oligopeptide chains composed of *R* residues, that is, of a configuration opposite to that of the initiator. An opposite effect is anticipated in the case of enantiomorphous pleated-sheet formation because an *S* initiator will integrate straightforwardly within the  $\beta$ -sheets composed from *S* strands (Figure 13b), whereas it will engender asymmetric hindrance and rate impediment in the growth of *R* strands (Figure 13c). The operation of the hindrance mechanism in the formation of rippled *ap*  $\beta$ -sheets was reported in the polymerization of (*RS*)-Phe-NCA crystals.<sup>[12]</sup>

The above-described experimental results from the polymerization of either racemic Val-NCA or racemic Leu-NCA, first dissolved in water and then treated with 25% enantiopure initiator, showed a reversal in the *ee* value of the long oligopeptides with respect to that of the short ones (Figure 10, left), a result in keeping with the formation of

rippled *ap*  $\beta$ -sheets. A comparison between the symmetrical chain elongation in the presence of an achiral initiator and the inhibition in chain elongation of an *S* strand introduced by an *S* initiator linked at the C terminus of an adjacent *R* strand ( $R_S$ -*S*-OMe) is modeled in Figure 14.

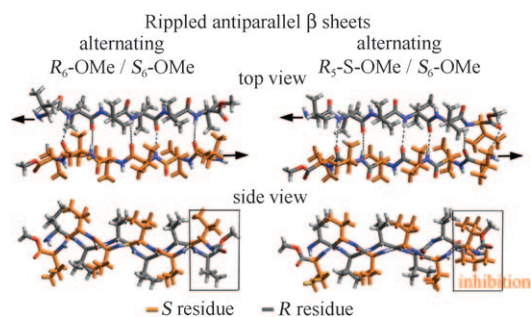


Figure 14. Top and side views of rippled *ap*  $\beta$ -sheets composed of alternating *R* and *S* strands with an achiral initiator (left) and with an *S*-Val-OMe initiator (right) that causes growth impediment due to steric hindrance.

Additional evidence was provided by a comparison between the distributions of the homochiral oligopeptides obtained from the polymerization of enantiopure *S*-Val-NCA in water initiated with either the *R*- or *S*-Val-OMe initiators, but otherwise under same conditions. The polymerization of enantiopure monomers can yield only the pleated  $\beta$ -sheets. MALDI-TOF MS analysis of the oligopeptides clearly demonstrates (Figure 15) that, beyond octamers, after the self-assembly into pleated  $\beta$ -sheets, the *S* oligopeptides obtained with *S*-Val-OMe are in excess over those obtained with *R*-Val-OMe; this result is in keeping with the formation of pleated *ap*  $\beta$ -sheets and is in contrast with the results obtained in the polymerization of racemic monomers. No

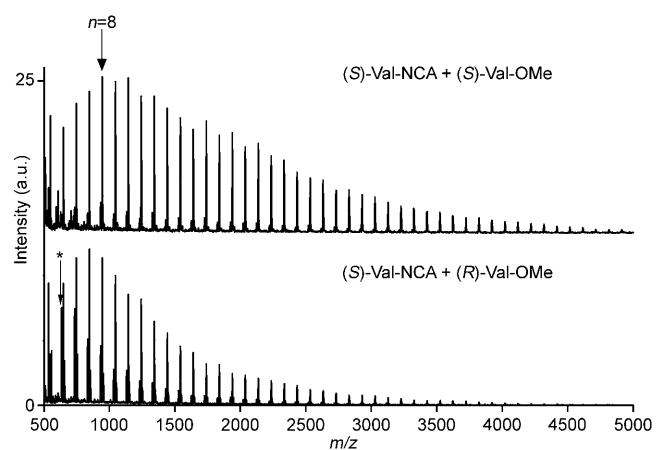


Figure 15. MALDI-TOF mass spectra of the oligopeptides obtained from the polymerization in water of *S*-Val-NCA with a) *R*-Val-OMe and b) *S*-Val-OMe initiators. The signal corresponding to the octapeptides is indicated by an arrow. In (b), there are relatively large amounts of short ( $n = 5$ – $8$ ) oligopeptides initiated by hydrolyzed Val-NCA, labeled with \*; this is in keeping with slower polymerization.

steric hindrance by the initiator linked at the C terminus is anticipated in parallel  $\beta$ -sheets, be they racemic or pleated, since this group will be located far away from the  $\text{NH}_2$  growing chain ends.

Another factor to be taken into consideration is a possible kinetic effect that might influence the *ee* value of isotactic peptides as a function of length. On one hand, the enantiopure initiators exert an asymmetric induction in the early stages of the reaction to enrich the solution with short oligopeptides composed from residues of the same handedness, but on the other hand, the solution is depleted of monomers of opposite handedness. As a result of the complexity of the polymerization process, it is difficult to evaluate the role of this kinetic effect. However, if the kinetic effect were responsible for the dramatic reversal in the *ee* value as a function of length for the polymerization with 25% initiator, we should have observed a related effect in the reactions with 5 and 10% initiator. Under the latter conditions, the *ee* value decreased gradually for the longer oligopeptides, but no reversal in *ee* value was observed (Figure 10). These results are clearly dependent on the nature of the templates formed at different concentrations of initiator. With 5 and 10% initiator, the templates also contain heterochiral oligopeptide chains, but comprise block sequences of homochiral residues that compel the chains to assemble in motifs that are very different from those of the rippled  $\beta$ -sheets formed with 25% initiator.

## Conclusion

The formation of long hydrophobic oligopeptides of homochiral sequence in the polymerization of racemic NCA monomers, in the presence of initiator, in water, and in the absence of enzymes, is demonstrated. Although pure NCAs are unstable derivatives of  $\alpha$ -amino acids, they have been proposed as possible intermediates for the formation of the early peptides.<sup>[26–30]</sup>

The generation of isotactic peptides comprises several steps that must operate in tandem. The present mechanism suggests that the simple formation of short racemic  $\beta$ -sheets and their operation as efficient stereoselective templates for the formation of isotactic peptides might suggest a plausible scenario by which the homochiral peptides emerged prior to the early enzymes. One of the important results in this study is that, although the templates can be composed of different racemic mixtures of short isotactic and atactic peptides comprising four to six residues and depending upon the initial concentration of the initiator, they can still exert regio-enantioselection in the chain-elongation processes. Such a mechanism has great advantages over the theoretical model proposed by Wald<sup>[31]</sup> of using  $\alpha$ -helices as templates for the spontaneous formation of long isotactic peptides,<sup>[32]</sup> because spontaneous self-assembly into helices would require the formation of peptides that have at least eight residues of the same handedness before they can exert asymmetric induction in the elongation of the peptide chains. The relative

ease of formation of the racemic  $\beta$ -sheets and their role as efficient templates in the generation of homochiral peptides suggests that they might have emerged prior to the  $\alpha$ -helices or the pleated  $\beta$ -sheets<sup>[33]</sup> in times of early evolution.

Studies on the design of other synthetic routes for the formation of homochiral peptides from racemic  $\alpha$ -amino acids are under current investigation.

## Experimental Section

### Materials

*N*-Carboxyanhydrides of valine and leucine: Val-NCA and Leu-NCA were prepared according to the method of Daly and Poché, with minor adjustments.<sup>[34]</sup> Finely ground *R*-Val or *R*-Leu (1 mmol, 0.5 equiv) and *S*-Val or *S*-Leu ( $d_8$  or  $d_{10}$ , 98%, Cambridge Isotope Laboratories; 1 mmol, 0.5 equiv) were suspended in dry THF and heated to reflux under argon. Solid triphosgene (0.8 mmol, 1.2 equiv) was added and after 0.5 h triphosgene portions (0.4 mmol, 0.6 equiv) were consecutively added every 0.5 h until a clear solution was obtained (2 or 3 portions were usually needed). The reaction was then continued for an additional hour. The clear solution was allowed to warm to room temperature and the THF was evaporated under reduced pressure.  $\text{CH}_2\text{Cl}_2$  (approximately 5 mL) was added and then hexane (about 50 mL) was added with mixing. A white precipitate appeared almost immediately; the suspension was cooled to 4°C for 2–3 h and then the crystals were filtered off. The small needle-like crystals of NCA were characterized by FTIR spectroscopy.

*Methyl esters of amino acids*: The free amine was prepared from commercially available monohydrochlorides of the amino acid methyl ester (Sigma) by suspending the material in dry  $\text{CH}_2\text{Cl}_2$  and bubbling with ammonia gas for a few minutes. The resulting solid  $\text{NH}_4\text{Cl}$  was filtered off and the  $\text{CH}_2\text{Cl}_2$  was removed by evaporation.

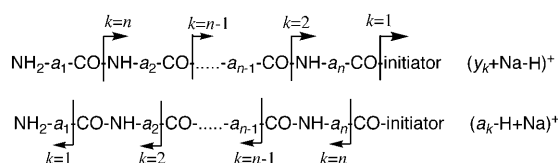
**Polymerization procedure**: Val-NCA or Leu-NCA (10 mg) was weighed into a microcentrifuge tube and dissolved in water (1 mL). The appropriate amount of *n*-butylamine or amino acid methyl ester was added after 5 min for Val-NCA and 1 min for Leu-NCA. The reaction was stirred vigorously for 24 h. The tubes were then subjected to centrifugation and the supernatant was carefully decanted and filtered to remove any residual precipitate. The precipitate and the supernatant were dried by lyophilization.

**MALDI-TOF mass spectra and analysis**: For sample preparation, a small amount of the sample (<1 mg) was placed into a polypropylene microcentrifuge tube and dissolved in trifluoroacetic acid (TFA; 20  $\mu\text{L}$ ). THF (80  $\mu\text{L}$ ) was then added. A volume (0.5  $\mu\text{L}$ ) of a 1:1 (v/v) mixture of the matrix (dithranol) solution in chloroform and a saturated solution of NaI in THF was placed on the target plate and dried. The solution to be analyzed (0.5  $\mu\text{L}$ ) was then deposited. MALDI-TOF positive-ion mass spectra were obtained in reflector mode with a Bruker Reflex III instrument equipped with an  $\text{N}_2$  laser. Mass spectra resulted from a signal average of at least several hundred laser shots on different spots of the target, to get reliable statistics about the ion peaks. Mass assignments of Na-cationized oligopeptides were made by using both the *m/z* values and the isotopic distributions. The following notation code is used for the peptide molecules: oligopeptide (*h,d*) assigns all molecules composed of *h* residues of *R* configuration (protonated) and *d* residues of *S* configuration (deuterated), with  $n = h + d$  being the total number of repeat units. The ionization yield is expected to be very similar for oligopeptides (*h,d*) of the same length *n*, due to their similar chemical properties and identical  $\text{Na}^+$ -ion affinity. One proof is given by a random polymerization for which the relative abundance of the different Na-cationized oligopeptides (*h,d*) of the same length perfectly fitted the binomial law. In addition, similar detection efficiencies are expected, due to very close masses and velocities in the TOF analysis. Thus, the ion intensities of the different diastereoisomeric oligopeptides (*h,d*) of the same length are directly and reliably comparable. The relative mole fraction of each type of oligopeptide (*h,d*) was obtained by dividing the intensity of the signals from a particular

molecule by the total intensity of the signals from all molecules of the same length  $n$ . For example, the relative abundance of tetrapeptide (1,3), composed of one  $R$  (protonated) and three  $S$  (deuterated) residues, was calculated according to Equation (1):

$$\text{Mole fraction of (1,3)} = \frac{\text{intensity of (1,3)}}{\text{intensity of (4,0)+(3,1)+(2,2)+(1,3)+(0,4)}} \quad (1)$$

MALDI-TOF-TOF spectra were obtained from an Applied Biosystems 4700 Proteomics instrument by using a time-ion selector over a mass window ( $\pm 3$  u) centered on the first isotope. Fragmentation of these ions by metastable decomposition and/or collision-induced dissociation ( $N_2$ ,  $2 \times 10^{-7}$  Torr, ion energy = 1 keV) showed that two main fragmentation series are produced for all of the initiators. These two series comprise either the  $N$  or the  $C$  terminus of the oligopeptide and are  $Na^+$  cationized (Scheme 2).



Scheme 2. The two main fragmentation series observed for the  $Na^+$ -cationized oligopeptide ions. These are referred to as the  $y$ -type and  $a$ -type series.

The  $y$ -type fragmentation series  $[y_k+Na-H]^+$  allows, typically, the exploration of the sequence of residues at the  $N$  terminus up to the half-way point. The  $a$ -type fragmentation series  $[a_k-H+Na]^+$  allows the exploration of the sequence at the  $C$  terminus, also over the length of half of the oligopeptides. Thus, both series have to be used to get sequence information. In all MALDI-TOF-TOF experiments, the number of laser shots was typically 10000 on 50 different spots on the target. This measurement allows us to obtain reliable statistics on the ion intensities.

## Acknowledgements

This work was supported by the Israel Science Foundation, the Clore Center for Biological Physics, and The Helen & Milton A. Kimmelman Center for Biomolecular Structure & Assembly. G.B. thanks Le Conseil Regional Ile-de-France and UPMC. We thank Dr. Alla Shainskaya and her team from the MS laboratory of the Weizmann Institute of Science.

- [1] S. Fox, *J. Chem. Educ.* **1957**, *34*, 472–479.
- [2] J. L. Bada, S. L. Miller, *Biosystems* **1987**, *20*, 21–26.
- [3] V. A. Avetisov, V. I. Goldanskii, V. V. Kuzmin, *Dokl. Akad. Nauk SSSR* **1985**, *282*, 115–120.
- [4] V. I. Goldanskii, V. A. Avetisov, V. V. Kuzmin, *FEBS Lett.* **1986**, *207*, 181–183.

- [5] V. Avetisov, V. Goldanski, *Proc. Natl. Acad. Sci. USA* **1996**, *93*, 11435–11442.
- [6] L. E. Orgel, *Nature* **1992**, *358*, 203–209.
- [7] P. Franck, W. A. Bonner, R. N. Zare in *Chemistry for the 21st Century* (Eds.: E. Keinan, I. Schecter), Wiley-VCH, Weinheim, **2000**, pp. 175–208, and references therein.
- [8] A. Brack, *Chem. Biodiversity* **2007**, *4*, 665–679, and references therein.
- [9] M. Blocher, T. Hitz, P. L. Luisi, *Helv. Chim. Acta* **2001**, *84*, 842–847.
- [10] T. Hitz, M. Blocher, P. Walde, P. L. Luisi, *Macromolecules* **2001**, *34*, 2443–2449.
- [11] J. G. Nery, G. Bolbach, I. Weissbuch, M. Lahav, *Chem. Eur. J.* **2005**, *11*, 3039–3048.
- [12] G. J. Nery, R. Eliash, G. Bolbach, I. Weissbuch, M. Lahav, *Chirality* **2007**, *19*, 612–624.
- [13] R. Eliash, J. G. Nery, I. Rubinstein, G. Clodic, G. Bolbach, I. Weissbuch, M. Lahav, *Chem. Eur. J.* **2007**, *13*, 10140–10151.
- [14] I. Rubinstein, R. Eliash, G. Bolbach, I. Weissbuch, M. Lahav, *Angew. Chem.* **2007**, *119*, 3784–3787; *Angew. Chem. Int. Ed.* **2007**, *46*, 3710–3713.
- [15] R. A. Illos, F. R. Bisogno, G. Clodic, G. Bolbach, I. Weissbuch, M. Lahav, *J. Am. Chem. Soc.* **2008**, *130*, 8651–8659.
- [16] H. R. Kricheldorf, *Angew. Chem.* **2006**, *118*, 5884–5917; *Angew. Chem. Int. Ed.* **2006**, *45*, 5752–5784.
- [17] L. Pauling, R. B. Corey, *Proc. Natl. Acad. Sci. USA* **1953**, *39*, 253–256.
- [18] T. Srikrishnan, N. Winiewicz, R. Parthasarathy, *Int. J. Pept. Protein Res.* **1982**, *19*, 103–130.
- [19] B. Lotz, *J. Mol. Biol.* **1974**, *87*, 169–180.
- [20] S. Munoz-Guerra, J. Puiggali, A. Rodriguez, J. A. Subirana, *J. Mol. Biol.* **1983**, *167*, 223–225.
- [21] A. V. Kajava, *Acta Crystallogr. Sect. D* **1999**, *55*, 436–442.
- [22] J. H. Fuhrhop, M. Krull, G. Büldt, *Angew. Chem.* **1987**, *99*, 707–708; *Angew. Chem. Int. Ed. Engl.* **1987**, *26*, 699–700.
- [23] Similar kinetic effects can also account for the abundant formation of racemic crystals, particularly among the hydrophobic amino acids in nature, in comparison with conglomerates of enantiomorphous crystals.
- [24] J. G. Nery, G. Bolbach, I. Weissbuch, M. Lahav, *Angew. Chem.* **2003**, *115*, 2207–2211; *Angew. Chem. Int. Ed.* **2003**, *42*, 2157–2161.
- [25] D. M. Chung, J. S. Nowick, *J. Am. Chem. Soc.* **2004**, *126*, 3062–3063.
- [26] A. Brack, *Biosystems* **1982**, *15*, 201–207.
- [27] C. Huber, G. Wächtershäuser, *Tetrahedron Lett.* **2003**, *44*, 1695–1697.
- [28] D. Hafenbradl, M. Keller, G. Wächtershäuser, K. O. Stetter, *Tetrahedron Lett.* **1995**, *36*, 5179–5182.
- [29] A. Commeyras, H. Collet, L. Boiteau, J. Taillades, O. Trambouze, H. Cottet, J.-P. Biron, R. Plasson, L. Mion, O. Lagrille, H. Martin, F. Selsis, M. Dobrijevic, *Polym. Int.* **2002**, *51*, 661–665.
- [30] I. Weissbuch, L. Leiserowitz, M. Lahav, *Top. Curr. Chem.* **2005**, *259*, 123–165.
- [31] G. Wald, *Ann. N. Y. Acad. Sci.* **1957**, *69*, 352–368.
- [32] Such a model has not yet been proved experimentally in the polymerization of racemic amino acid activated derivatives.
- [33] A. Brack, G. Spach, *J. Mol. Evol.* **1979**, *13*, 35–46.
- [34] W. H. Daly, D. Poché, *Tetrahedron Lett.* **1988**, *29*, 5859–5862.

Received: July 21, 2008  
Published online: October 27, 2008